Defence Research and Development Canada
Recherche et développement pour la défense Canada

The theory of internal wave wakes

James K.E. Tunaley

This report was completed in March 2012.

Defence R&D Canada – Ottawa

Contract Report
DRDC Ottawa CR 2012-119
June 2012

Canada

The theory of internal wave wakes

James K.E. Tunaley

Prepared By:
London Research and Development Corporation
114 Margaret Anne Drive,
Ottawa, Ontario
K0A 1L0
Contractor's Document Number: 2012-03-001
Contract Project Manager: J.K.E. Tunaley, 613-839-7943
PWGSC Contract Number: W7714-4500869967
CSA: Paris W. Vachon, Scientific Authority, 613-991-2584

This report was completed in March 2012.

Defence R&D Canada – Ottawa

Contract Report
DRDC Ottawa CR 2012-119
June 2012

Scientific Authority

Original signed by Paris W. Vachon

Paris W. Vachon

Scientific Authority

Approved by

Original signed by Caroline Wilcox

Caroline Wilcox

Head, Radar Applications and Space Technologies

Approved for release by

Original signed by Chris McMillan

Chris McMillan

Chair, Document Review Panel

Abstract

In practice, maritime surveillance includes the detection and observation of surface ships and possibly submarines, which create various types of disturbances on the sea surface. The disturbances, which form a wake, can sometimes be detected by radar, which responds to surface flows and height variations as well as slicks. The radar may be on a terrestrial platform, on an aircraft or on a spacecraft. This report focuses on the characteristics of the surface flows created by the generation of internal waves by a moving body. The treatment involves the calculation of crest patterns on the surface; it is demonstrated that these can be derived simply from the numerical solutions of a second order differential equation that describes internal waves in an internal layer with a prescribed Brunt-Väisälä profile. Though other workers have performed similar calculations, they do not describe the methodology and its details.

The numerical approach is based on a determination of eigenvectors and their eigenvalues. These represent the profiles of the waves in the layer and the horizontal wave vectors respectively. The extension to a determination of the wake wave amplitudes is outlined and the potential for the detection of submarines is discussed.

This method, which embodies simple physical models, is designed to be straightforward and expected to be a precursor to an efficient full simulation of internal wave wakes.

Résumé

Dans la pratique, la surveillance maritime comprend la détection et l'observation de navires de surface et, éventuellement, de sous-marins, qui créent divers types de perturbations à la surface de la mer. Les perturbations, qui forment un sillage, peuvent parfois être détectées par radar, qui réagit aux variations de la circulation et de la hauteur de l'eau en surface, de même qu'à la présence de nappes. Le radar peut être sur une plate-forme terrestre ou à bord d'un aéronef ou d'un engin spatial. Le présent rapport porte sur les caractéristiques de la circulation de l'eau en surface, résultant des ondes internes générées par un corps en mouvement. Le traitement des données comprend le calcul des modes d'oscillation des crêtes à la surface; il est démontré que ceux-ci peuvent être dérivés simplement de solutions numériques d'une équation différentielle de second ordre décrivant les ondes internes dans une couche interne au moyen du profil de fréquence de Brunt-Väisälä prescrit. Bien que d'autres chercheurs aient exécuté des calculs similaires, ils ne décrivent pas la méthodologie en détail.

L'approche numérique est basée sur une détermination des vecteurs propres et de leurs valeurs propres. Ceux-ci représentent respectivement les profils des ondes dans la couche et les vecteurs d'ondes horizontaux. Le présent rapport donne un aperçu d'une extension du modèle s'appliquant au calcul de l'amplitude des ondes de sillage et traite des capacités de détection des sous-marins.

Cette méthode, qui incorpore des modèles physiques simples, est conçue pour être explicite et devrait faciliter une simulation efficace et complète des sillages d'ondes internes.

Executive summary

The theory of internal wave wakes

James K.E. Tunaley; DRDC Ottawa CR 2012-119; Defence R&D Canada – Ottawa; June 2012.

Introduction: As well as assisting ship detectability in radar imagery, wakes offer the potential for extracting useful information about the ship and the ocean environment. Also, they can be used to cross validate existing information. The wake from a surface ship is often observed in satellite borne Synthetic Aperture Radar (SAR) and it seems likely that observable wakes are created by submarines, at least under favourable conditions. A necessary condition is the presence of an oceanic internal layer, which can support internal waves. The internal waves due to a moving source, either on the surface or submerged, create a pattern of crests, which typically comprise divergent waves. This is a consequence of fundamental hydrodynamic processes, which produce both horizontal flows at the surface and a small disturbance of the sea height. In turn, these affect the radar scattering by perturbing the propagation of Bragg waves.

This report focuses on the modeling of the hydrodynamic wake using simple physical principles that can be understood by a reader with only limited familiarity with hydrodynamics. It represents an updated version of previous work by the author and others.

Results: The basic theory of internal wave wake modeling is addressed. A detailed example using a practical Brunt-Väisälä vertical profile is illustrated. The crest pattern due to a moving source within the layer is derived and this resembles that for an early simplified model due to Keller and Munk. Some comparisons are made with the discrete layer model. Finally the extension to modeling the surface flow velocities from a distribution of sources is discussed. It seems likely that internal wave wakes from submarines could be observable especially under conditions where the surface mixing is very thin or absent, such as can occur in the Straits of Gibraltar.

Significance: Our capability to detect submarines using radar is partly contingent upon an understanding of the production of internal wave wakes. An understanding greatly assists evaluating the utility of SAR wakes in Maritime Domain Awareness, especially in wide area surveillance from space. Such understanding is important both for observing red force vessels and for minimizing the signature of blue force ships and submarines.

Future plans: This report is a precursor to the development of an efficient software modeling package, which includes surface perturbations and radar scattering. A simulation will be useful for internal wake characterization. An immediate goal is to establish more precisely the conditions under which submarines are detectable by radar. This includes an extension to internal layer vertical profiles with multiple peaks and to unsteady wakes.

Sommaire

The theory of internal wave wakes

James K.E. Tunaley ; DRDC Ottawa CR 2012-119 ; R & D pour la défense Canada – Ottawa; juin 2012.

Introduction : En plus de favoriser la capacité de détecter les navires dans les images radar, les sillages offrent la possibilité d'extraire de l'information utile sur les navires et le milieu océanique. Ils peuvent également servir à contre-valider des renseignements existants. Le sillage d'un navire de surface est souvent observé par radar à synthèse d'ouverture (RSO) à bord d'un satellite, et il apparaît probable que des sillages observables soient produits par des sous-marins, du moins dans des conditions favorables. La présence d'une couche océanique interne, qui peut comporter des ondes internes, est une condition essentielle. Les ondes internes produites par une source en mouvement, à la surface ou submergée, créent un mode d'oscillation des crêtes, comportant habituellement des ondes divergentes. Il s'agit d'une conséquence des processus hydrodynamiques fondamentaux, qui produisent à la fois des mouvements horizontaux à la surface et de petites perturbations de la hauteur de la mer. À leur tour, ces mouvements influencent la diffusion radar en perturbant la propagation des ondes de Bragg.

Le présent rapport porte sur la modélisation du sillage hydrodynamique en utilisant des principes physiques simples, faciles à comprendre par un lecteur possédant des connaissances limitées de l'hydrodynamique. Il s'agit d'une version actualisée de travaux antérieurs réalisés par l'auteur et d'autres collègues.

Résultats : Le rapport présente la théorie de base de la modélisation du sillage d'ondes internes. Il présente également un exemple détaillé et pratique d'un profil vertical de Brunt-Väisälä. Le mode d'oscillation des crêtes, produit dans la couche par une source en mouvement, est représenté et ressemble à celui d'un ancien modèle simplifié élaboré par Keller et Munk. On fait certaines comparaisons avec le modèle de couches distinctes. Enfin, on examine l'extension de la modélisation des vitesses de circulation en surface selon une répartition des sources. Il apparaît probable que les sillages d'ondes internes produits par des sous-marins pourraient être observables, particulièrement lorsque la couche de mélange des eaux de surface est très mince, voire absente, comme cela peut se produire dans le détroit de Gibraltar.

Importance : Notre capacité de détection des sous-marins au moyen du radar est en partie subordonnée à notre compréhension de la production de sillages d'ondes internes. Cette compréhension facilite grandement l'évaluation de l'utilité des sillages déterminés par RSO pour la connaissance de la situation maritime, particulièrement pour la surveillance d'une vaste région depuis l'espace. Une telle compréhension est importante tant pour l'observation de navires de la force rouge que pour atténuer la signature de navires et de sous-marins de la force bleue.

Perspectives : Le présent rapport est le prélude à l'élaboration d'un progiciel de modélisation efficace, comprenant les perturbations en surface et la diffusion radar. Une simulation sera utile pour la caractérisation de sillages d'ondes internes. Dans l'immédiat, le but consiste à établir de façon plus précise les conditions favorables à la détection de sous-marins par radar. Cela inclut

une extension du modèle s'appliquant aux profils verticaux de la couche interne avec pics multiples, ainsi qu'aux sillages instables.

This page intentionally left blank.

Table of contents

List of figures

Acknowledgements

Thanks are due to Paris W. Vachon for his interest and encouragement in this important topic.

This page intentionally left blank.

1 Introduction

The reader can find mathematical details in the Annexes but most of the central physical results are located in the main text; the Annexes are only necessary for those wishing to pursue further information or simulation.

1.1 Background

Maritime security relies on Maritime Domain Awareness (MDA), which involves ocean surveillance using a multiplicity of different sensor systems. The requirement is for persistent surveillance out to 2000 nmi from the coasts. The costs are likely to be prohibitive unless sensors are located on board orbiting satellites. Passive sensors tend to be limited to daylight or rely on transmissions from ocean going vessels. This implies that passive sensors cannot fulfill the requirement, especially in northern waters during winter darkness. Space-borne active sensors are based on microwave radar, such as the Synthetic Aperture Radar (SAR) on RADARSAT-2, which operates at microwave frequencies in C-band.

SAR is well suited to wide area maritime surveillance and forms the basis of Canada's Polar Epsilon project. Radar returns from ships can be identified and their locations determined accurately; the data can be integrated with those from other sources to enhance the Recognized Maritime Picture (RMP). As well as ship returns, ship wakes are often visible in a radar image. In the open ocean, where large surface vessels tend to travel at service speeds of 20 knots or more, the frequency of wake visibility is likely to be more than 50 percent [1], [2]. This offers the potential for extracting useful information from the wake. For example, the position of a wake in a radar image is very close to its true position. However, the return from a moving ship is Doppler shifted and the SAR processor interprets this as a displacement of the ship image in the cross-range direction. The displacement is proportional to the ship speed and allows an independent estimate of ship speed.

There are several types of ship wakes in both the hydrodynamic sense and the radar sense. The most common is the turbulent wake that typically appears as a narrow dark streak along the ship track. This can be employed to estimate the ship course. Other types of wake are a result of surface gravity waves excited by the passage of the vessel. These can be of the Kelvin type, which is created by flows around the ship hull that are stationary in a frame of reference traveling with the ship. Another type is associated with unsteady flows in the ship frame; these can be created by the reflection of ambient waves from the hull, by ship motion (particularly heave and pitch) and by excitations at the propeller blade frequency. In the case of the turbulent wake, the author believes that the effect on the radar is primarily through horizontal surface flows, but others invoke slicks or surfactants brought to the surface by the ship's propellers. For surface gravity waves, variations in surface height can also be important [3].

Internal waves can be created by objects moving near an internal layer and naturally, by water flowing over obstacles on the ocean floor [4], [5]. Internal wave wakes due to surface ships have been observed in SAR imagery [6] but, though there has been speculation that internal wave wakes should be created by submarines, there is no credible unclassified record of such observation. There are several reasons why this is to be expected. Firstly, there is concern that the

national interest may not be well served by an admission that submerged submarines can be detected by SAR. Secondly, the mechanisms for the production of internal wave wakes have not been fully explored. However, as time passes, various foreign entities have gained access to SAR data; it is increasingly important to determine whether internal wave wakes from submarines are detectable by radar and under what circumstances. The purpose is as much for the protection of our own assets as for locating those of enemies.

It should be appreciated that microwave radar signals cannot penetrate the ocean surface so that, though there may exist large amplitude waves at depth, we are only concerned with the manifestation of internal waves at the water surface.

1.2 Internal layers

Internal waves may be produced in the ocean when stratification of the water density exists in horizontal layers [4]. An example is when fresh water overlies salt water in a fjord so that there is an abrupt jump in the density as a function of depth. An object moving close to the horizontal interface between the two bodies of fluid will excite waves on the interface just as waves are produced when a ship moves on the surface interface between water and air. In the case of the air-water interface, a Kelvin wake is created with a distinct crest pattern. Similarly, a wake of internal waves is produced with its own set of characteristic crest patterns. The presence of a wake can sometimes be used to confirm the observation of a ship or even as a ship detector.

Vertical variations in temperature and salinity can lead to density stratification if certain conditions are met with respect to stability [7]. If the temperature increases with depth or the salinity decreases with depth, the fluid becomes unstable and mixing will take place; this implies that stratification cannot exist. Stable layers are most likely to occur in the tropics, where the surface water temperature is warm, in the arctic, where melting ice can create fresh water layers and near estuaries.

Stratification in density, which is described by its vertical profile, depends on the season and geographic location as well as the wind and ambient wave conditions that control mixing in the upper ocean. The upper few meters are often well mixed and significant departures from a more or less constant density, if they occur at all, may start a few meters from the surface or up to several hundred meters. The depth range over which the stratification takes place is also quite variable.

Waves created within an internal layer tend to propagate slowly compared with surface gravity waves and the disturbance tends to decrease rapidly away from the layer as a function of vertical distance. In the vertical plane the particle paths in a simple sinusoidal surface gravity wave are close to circular in shape. In contrast, the paths of particles in an internal wave that is propagating horizontally are close to elliptical. Moreover, the ellipses are very elongated in the horizontal direction so that the displacement at the ocean surface is negligible in almost all cases of practical interest [4]. However, the horizontal surface velocities can be significant for radar detection.

For example, radar, such as RADARSAT-2 operating at microwave frequencies in C-band and with angles of incidence about 30º, responds to Bragg waves with a group velocity of about 14 cm/s. Therefore surface speeds of even a few centimetres per second will cause refraction of the

Bragg waves, as recognized by Alpers [8]; the changes in direction of propagation as well as transfers of energy between the waves and the flows may render both naturally occurring internal waves as well as wakes visible in a radar image [9].

Ideally, the vertical profile would be known from sounding equipment, but this is usually not practical for general surveillance and reliance must be placed on ocean modeling. Because of uncertainties in the parameters of the layers as well as a lack of knowledge of the details of the object causing a disturbance, we consider simplified cases. Unnecessary theory is avoided by taking as given that the surface wave field is decoupled from the internal wave field and that the water is incompressible and inviscid [4]. These assumptions are expected to be valid within the context of this report.

The simplest case is that of an abrupt jump in density. This corresponds to a stable situation where fluid of lesser density lies over fluid of greater density, which, as noted already, may occur in a fjord. The source of a disturbance may lie either above or below the interface. In each case, waves can be induced on the interface, which moves up and down. The depth of the layer and the distances of the sources from the layer are clearly important factors.

A diffuse layer is described in terms of the rate of change of density with depth. This leads to a characteristic frequency called the Brunt-Väisälä (B-V) frequency, $N(z)$, where z is the depth. This frequency is the maximum angular frequency at which internal waves can propagate at that depth. In the open ocean N is typically less than 0.02 rad/s [4], [7] though it can be much greater in a fjord. As a function of depth, the B-V frequency often increases sharply to a maximum and then falls off slowly. However the B-V profile may exhibit multiple peaks. In fjords, the layer may be quite thin and the change in density can be abrupt; this leads to much higher B-V frequencies but concentrated over a small depth range.

The propagation of internal waves was studied by Mowbray and Rarity in the laboratory [10] and by others: [11], [12] and [13]. Internal waves can propagate vertically as well as horizontally but their three-dimensional propagation is anisotropic.

This suggests that, for a typical B-V profile, internal waves are likely to be trapped in the horizontal layers of high N. The behaviour resembles that of a waveguide in electromagnetic theory. Within a layer and when the angular frequency is less than N, waves are reflected at upper and lower boundaries of the layer and effectively propagate horizontally. Outside of these boundaries the disturbance tends to fall off exponentially. Thus there are a number of modes. The simplest is when the entire layer moves up and down; this is called sinuous motion. Modes in which the upper and lower surfaces move in anti-phase are called varicose modes. Hybrid modes exist in which the upper and lower boundaries move in phase but the interior moves in anti-phase.

A source that moves above or below the layer primarily produces sinuous movement while a source moving within the layer produces a combination of sinuous and varicose movement. It is important to note that the ability of internal waves to propagate vertically (which results in horizontally propagating “waveguide” modes) implies that an internal layer may allow any disturbance at depth to propagate to the top of the layer, which is often close to the surface. Therefore the disturbance is quite likely to be visible to radar looking at the sea surface, just as for surface ships. The question is not so much as to whether a sub-surface source can be detected by its internal wave wake, but under what circumstances.

1.3 Ship models

In an idealized model, the passage of a ship moving smoothly through the water creates a flow pattern that is stationary in the ship frame of reference. The actual flow deviates from the ideal because water sticks to the hull and this creates a turbulent boundary layer, which is unsteady. Fortunately this layer is quite thin compared with typical hull dimensions so that a stationary flow is a reasonable approximation if the hull is notionally extended to the edge of the boundary layer. The boundary layer detaches from the hull and creates a wake. This wake also has turbulent and unsteady, random components but, in the reference frame of the ship, the steady components of the flow around the hull and in the wake predominate. This is just as true for a submarine as for a surface ship.

It is further assumed that a disturbance can be represented by a fluid source or a collection of sources moving horizontally at the ship velocity, each source at constant depth, and all at the same constant velocity. Sinks are included as negative sources. The use of sources and sinks is a typical approach, which has been studied by Havelock in 1935 [14], and is still used [15], though other methods can be employed.

The flow can be described by streamlines or stream-tubes; the edge of the boundary layer is a stream-tube. The idea is to employ a distribution of sources and sinks that creates the same flow pattern as the hull and its wake. The sources generally lie near the bow of the hull that is being modeled; the net flow from the sources pushes the water and the stream-tubes away from the source. The sinks generally lie near the stern and pull water in. A suitable combination of sources and sinks can represent, at least in an approximate way, the flow around a real hull. However, there may be a difficulty in representing the flow near the stern. This is due to the effect of turbulence and the detachment of the boundary layer to form the wake. Wake formation tends to reduce the pressure on the hull near the stern and create a “form drag”.

When a vessel moves at constant velocity, the net force on it is zero. This implies that the propulsion system must compensate for all the drag forces by generating a sternward production of linear momentum in the wake. An equivalent view is that this momentum production compensates for the momentum carried forward by the water dragged along by the skin drag, the water pushed forward by the back-pressure at the stern (form drag) and the momentum of the internal and surface gravity waves. Moreover, because the movement of a ship does not introduce any fluid, the net source strength must be equal to the net sink strength.

The condition on the net source strength need not apply locally as sources and sinks can lie in the wake at large distances from the ship. This occurs when the wake carries away linear momentum associated with propeller thrust, which is needed to offset the drag. There is no mechanism to remove linear momentum from the wake except viscous dissipation at the ocean bottom or shore line. A broadening of the wake by turbulent diffusion has no effect on the total linear momentum that it carries because fluid entrainment does not involve external forces.

The simplest hull model comprises a single source and a single sink of equal magnitude. This might apply to an ideal ship of appropriate shape that travels at constant speed on or under a smooth ocean with no resistance. However, the situation is complicated by the presence of a wake: the entire wake can act as a sink. A surface ship is best modeled by a distribution of

sources with an equal number of sinks, some of which are located at very large distances in the wake (or at infinity). Effectively, this is the approach described by Havelock [14].

In the absence of an internal layer a submarine well below the surface may not experience wave-making resistance. Then, at constant velocity, the propeller thrust cancels the form and hull drag and the net production of linear momentum in the wake is close to zero. Another factor is the collapse of the turbulent wake due principally to mixing of the fluid by the propellers in the turbulent wake. This mixing creates a horizontal cylinder of fluid of more or less constant density within the stratified water. The cylinder is unstable because the upper part is denser than the surrounding medium and the lower part is less dense than the surrounding medium. The wake tends to collapse vertically while spreading out horizontally. The collapse produces "pancake" eddies in the horizontal plane and oscillations take place at a frequency close to the local B-V frequency. Therefore it is expected to be an efficient generator of internal waves, which damp the oscillations. However, in another point of view, the collapsing wake can be regarded as an extension of the ship. The distribution of sources and sinks can then contain strong Fourier components at the oscillation frequencies and these may be responsible for internal wave production.

In the case of a cylindrical submarine with a blunt bow, a single source might be sufficient to model the streamlines located near the bow. A distribution of sinks may be required near the stern but of significantly smaller magnitude. Some sources and sinks may correspond to the collapsing turbulent wake; some sinks will be at infinity. Another set of sources and sinks are necessary to represent the submarine sail and other appendages.

Once a suitable distribution of point sources and sinks has been established, it is possible to simulate a wake using a linear superposition of individual wakes, one from each source and sink.

Annex A provides some details about the point source in the frequency domain.

2 Wake theory

We are interested in the disturbance at the sea surface caused by the production of internal gravity waves associated with a surface ship or submarine. In principle, a component of the surface waves is due to the generation of waves at the air-water interface. If a surface vessel is moving slowly, this is usually quite small. If a submarine is at depth, the generation of an air-water surface gravity wave component is further reduced. An estimate of this latter component is possible but is beyond the scope of the report.

In addition it is assumed that the waves are generated by flows that are stationary in the frame of the ship. This implies that the wake pattern is also stationary in the ship frame. Thus the effects of ship motions associated with an ambient wave field are neglected. The turbulent wake, including the collapsing wake of a submarine, can be included (with the exception of its random turbulent components) by a distribution of sources and sinks. Unsteady sources and their wakes could make an important contribution towards wake visibility but again this is beyond the scope of the present report. They could be important for detection by radar as well as by methods involving underwater sensors.

The theory of wakes due to the excitation of surface waves from a moving ship has a long history beginning with the Kelvin wake. In general the theory must first address the crest pattern. This can be simplified by treating only the far wake. The near wake is likely to be very complicated because it is affected by details of the hull shape and texture, which determine the extent of turbulence in the boundary layer, and by wave breaking. Turbulence and wave breaking produce unsteady wakes, which are predominantly at small wavelengths. These waves are likely to decay rapidly because of viscous effects.

It turns out that the crest pattern of the far wake is best attacked by a frequency domain approach. This is appropriate because, during propagation in a dispersive medium, the shape of any disturbance tends to evolve into a sinusoid. Each crest is in the form of a line and its shape is determined entirely by the phase of that crest, the Doppler shift of component waves in the wake and by the distance traveled by the disturbance according to the group velocity. Therefore the problem merely requires the Doppler equation and the dispersion relation. For example, for the Kelvin wake, the flow is stationary in the ship frame, which is moving with velocity **U** relative to the ocean. The Doppler equation is then:

$$0 = \omega - \mathbf{k} \cdot \mathbf{U} \,, \tag{1}$$

where ω is the angular frequency of the waves in the ocean and **k** is the angular wave vector; the angular wave vector, **k,** lies in the horizontal plane and is two-dimensional. It is worth noting that, if this equation is divided by k, it becomes a condition on the phase velocity of the waves and that this can also be used as a basis for crest theory [7]. Thus along a crest, the phase velocity is equal to that component of the ship velocity parallel to the wave vector. The dispersion relation for surface gravity waves on deep water is well known and is provided in any elementary text, such as [7]; it is given by:

$$\omega^2 = gk\,, \tag{2}$$

where g is the acceleration due to gravity. These equations can be solved to yield the angle between the wave vector and the ship velocity as a function of k. The group velocity (being equal to $d\omega/dk$) can be found by differentiating the dispersion relation and this, together with the geometry, provides the propagation distance and position of a disturbance. The crest pattern for Kelvin and other wakes can be derived as shown in Annex B; the Kelvin pattern is illustrated.

The crest patterns derived by this method are quite realistic. This is because the water waves are highly dispersive. As noted, when a disturbance propagates away from its source, the waves rapidly become close to sinusoidal in shape, whatever their original shape. The general approach is analogous to a mathematical calculation using the steepest descents or saddle point methods; these types of methods are known to give unexpectedly accurate results over large domains in parameter space. In particular the crest patterns are reasonable even close to a ship.

The next problem after a determination of the crest pattern is to estimate the wave amplitudes. In the following discussion, a frequency domain approach is employed once again and dispersion relationships arise quite naturally as the effect of a source on an internal layer is determined. One approach is to find the disturbance from a fixed source oscillating with angular frequency ω_0, and then, by transforming to a moving system, the wake can be calculated [7]. In this report, an equivalent but simpler method is adopted. There are several possible options in the calculations but only basic scenarios of practical importance are considered here.

One of the first attempts to address internal wave wake production was due to Hudimac [16]. A two-layer ocean model with a discrete interface was adopted and crest patterns were derived. Unfortunately, for the low ship speed case, the transverse and divergent waves did not meet at the wake edge, which is a caustic as in the Kelvin wake pattern. This suggests that there was an error in his numerical algorithms. Later Miles [17] produced a theoretical treatment of internal waves generated by a horizontally moving source. He considered the two cases of a constant B-V frequency and a discrete interface. Approximate results for both a dipole source and a collapsing turbulent wake are given; these are asymptotic formulae and their domain of validity is not obvious.

Borovikov et al. [18], [19] adopted a Green's function approach to the estimation of internal waves generated by a moving source. This provided a plausible crest pattern, which included amplitudes, for a B-V frequency profile with a single broad peak. The treatment was mathematical and was not particularly transparent with respect to the physics. The authors claim that, for the most part, asymptotic solutions are adequate. However, it is still necessary to calculate a few eigenfunctions that represent the allowed vertical oscillations within the layer (as is illustrated later).

A much more satisfactory theory of crest patterns produced by a moving source of constant magnitude is due to Keller and Munk [20]. This approach was adopted by Dysthe and Trulsen [21] in a theoretical study, which included a comparison with experiments under a Norwegian program in 1988. The internal layer model was simplified; it consisted of a layer with a constant B-V frequency sandwiched between water of constant density. The predictions were in rough agreement with the observations. Surface flow amplitudes were estimated using a thin ship model

of the ship “Saebjorn” and these provided a surprisingly satisfactory agreement with the observed flow velocities. This approach has also been successfully exploited by Hogan et al. [6] to explain the observations of internal wake waves in the Loch Linnhe trials. These last authors calculated the crest patterns for the vertical profiles existing in the Loch. Their type of calculation will be repeated for a typical profile, but the method will be explained in detail, the utility of the crest pattern for maritime surveillance will be discussed and the extension to predicting the wave amplitudes will be addressed. The question of amplitudes has not been answered by [6] or [20].

2.1 The collapsing turbulent wake

Because the collapsing turbulent wake is both important and has received a great deal of attention, it is necessary to summarize the main features.

The initial studies were performed in the laboratory by Schooley and Stewart [22]. They found that the turbulent wake of a self-propelled submerged body is an efficient generator of internal waves and that the damping mechanism is principally viscosity and not turbulence.

A subsequent experimental study has been described by Wu [23]. The vertical fluid density gradient was approximately constant (the B-V frequency varied somewhat with fluid depth). He found that the wake collapse occurred in three stages: the initial, principal and final stages. In the first two stages the collapse is primarily a gravitational flow phenomenon. Viscous effects predominate in the final stage. The results were described in terms of non-dimensional numbers, such as the Froude and Richardson numbers. Wu attributed the generation of internal waves entirely to the initial stage of collapse. Moreover, the energy density of the waves was peaked at about 80% of the local B-V frequency; it cut off at the B-V frequency itself. These results are in accord with intuition. The rate of collapse in the initial stage was almost constant and controlled mainly by the Froude number.

Schooley and Hughes [24] continued to study the collapse. They note that various modes of oscillation exist and that the lowest mode (their Mode 1), which consists of an up and down sinuous motion, is unlikely to be excited. Similarly all their odd numbered modes (our even numbered modes) should be suppressed; varicose modes should predominate.

The collapse has been reviewed by Kao [25] and the theory was extended by him in 1976. The initial stage uses the linearized theory of Hartman and Lewis [26], which is not trivial. However, the authors suggest that non-linear theory is needed for an accurate modeling of the collapse in the initial stage. The initial stage occurs when $Nt < 2.5$, the principal stage when $3 < Nt < 25$ and the final stage when $Nt > 25$. Here t is the time, which is related to the vessel speed and the distance astern. The initial collapse stage can extend for hundreds of meters.

Other related works are in [27] to [34]. Robey [35] considers a towed sphere and finds that the sphere is effectively elongated by the separation bubble. He notes that there is an unsteady part of the internal wave field associated with non-stationary turbulence. The conclusions of all these workers tend to support the fundamental theory of wake collapse and wave generation.

More recent experiments have been described by Bonnier and Eiff [36]. These involve a towed sphere and focus on the unsteady aspects of wake collapse. As concluded by others, they find that

the transitions between the regimes are a function of the internal Froude number, rather than the Reynold's number. The internal Froude number is given by:

$$F = \frac{U}{Na}, \tag{3}$$

where a is the sphere radius in this case or characteristic dimension generally. For ships and submarines, this is likely to be of the order of 100 or more.

2.2 Waves on a discrete interface

The simplest model for an internal layer is an abrupt change in density at some depth, h, where the density changes from ρ_1 to ρ_2 with $\rho_2 > \rho_1$. The model has some shortcomings in that it applies strictly only in a few circumstances, such as in a fjord where fresh water may overlie salt water. However, it does serve as an introduction to internal wave wakes and can be useful to check orders of magnitude. The model is simplified to eliminate surface gravity waves, though this is not strictly necessary in practice because the dispersion relation for surface gravity waves (2) appears as a factor in the overall dispersion relation. To satisfy the boundary conditions, continuity of pressure and velocity across the interface are applied. The details are provided in Annex C. The waves on the internal interface are of course purely sinuous.

The model leads to the dispersion relation:

$$\omega^2 = \frac{(\rho_2 - \rho_1)gk}{\rho_2 + \rho_1 \coth(|\, h \,|\, k)}, \tag{4}$$

where g is the acceleration due to gravity. When the difference in the densities is very small, as occurs in practice and has been shown by Phillips [4], this can be simplified to:

$$\omega^2 = \frac{\delta g k}{1 + \coth(|\, h \,|\, k)}, \tag{5}$$

where δ is the fractional change in density across the internal interface, which is rarely more than 0.02.

The crest pattern is conveniently handled in terms of normalized variables [7]:

$$\Omega = \frac{\omega U}{\delta g}; \kappa = \frac{kU^2}{\delta g}; H = \frac{|\, h \,| \delta g}{U^2}, \tag{6}$$

where U is the source speed. It is easily verified that the normalized phase and group velocities, Ω/κ and $d\Omega/d\kappa$ are equal to the actual velocities normalized by U. It follows that the crest

patterns derived from the dispersion relation in normalized coordinates are valid for all source velocities with a coordinate scaling factor equal to $\delta g/U^2$ (as for H above). Because in practice δ is likely to be small, so is H, but Ω and κ are likely to be large.

The dispersion equation now becomes:

$$\Omega^2 = \frac{\kappa}{1 + \coth(\kappa H)}. \tag{7}$$

This can be plotted for various values of H as in Figure 1.

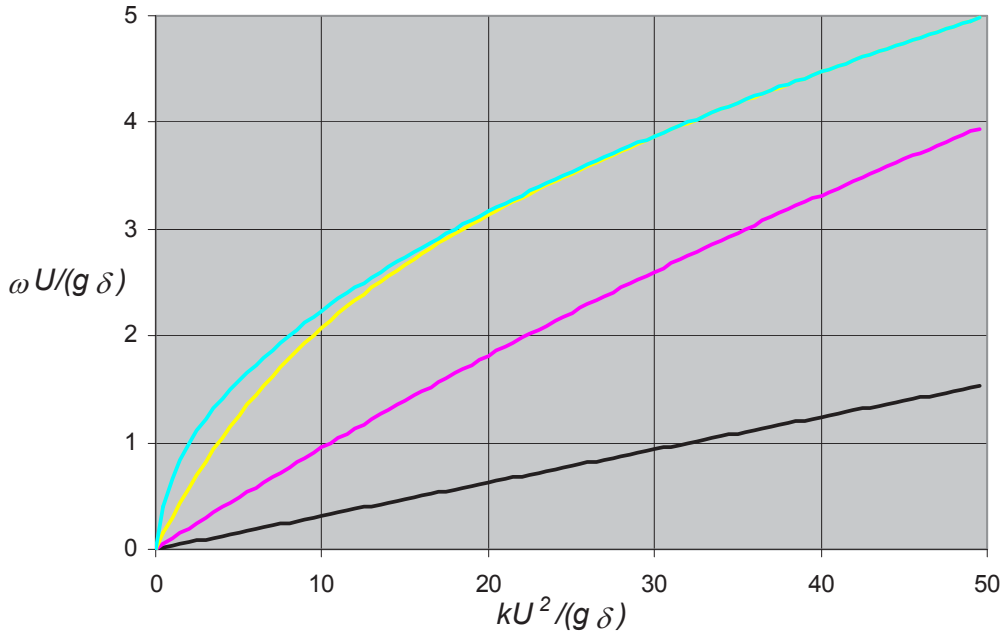

Figure 1: Dispersion relation for the discrete interface. H=0.001(—); H=0.01(—); H=0.1(—); H=1.0(—).

The range of values for κ has been chosen to be appropriate to a ship of size between 10 and 50 m moving at about 5 m/s. Such a source excites waves of similar wavelength. Values of H correspond to values of $\delta < 0.02$ and $h < 100$ m. When H is small, which corresponds to a layer at small depth or a weak layer or a source moving at high speed, the graph is almost a straight line so that the waves are practically dispersionless; therefore the wake resembles a two-dimensional analogue of the Mach cone from a supersonic aircraft.

An analysis of the dispersion relation for small k, where the slope is greatest and the graph is approximately straight, provides the maximum speed of the wake waves (in other words the

maximum phase and group velocities) and shows that the maximum wake half angle, $\beta_{\max}$, is given by:

$$\sin \beta_{\max} = \sqrt{\delta g h} / U = \sqrt{H} \ . \tag{8}$$

From Figure 1, for H = 0.001, the maximum phase and group normalized velocities are about 0.03. Therefore the half angle of the wake can be found either from this or from (8); the half angle for a source moving at 1 m/s is approximately 0.032 radians or about 1.8º. At 5 m/s, the wake half angle would be about 0.36º. As H increases, the plots are still straight near the origin, so that the wake waves of long wavelength are almost dispersionless but the maximum phase and group velocities increase.

It is important to note that in practical situations, the source is likely to be moving faster than the maximum speed of waves, which is equal to $H^{1/2}U$. Transverse waves in the crest pattern can only exist if these waves can travel at least as fast as the ship to satisfy the phase condition arising from (1). Therefore, as long as $H < 1.0$, there can be no transverse waves in the wake and the crest pattern is of the divergent type. In the following only $H < 1.0$ will be considered.

The method of calculating the crest pattern is described in Annex B. This requires the normalized phase and group velocities, which can be derived from (7):

$$\begin{aligned} C &= \frac{\omega}{kU} = \left(\kappa(1+\coth(\kappa H)\right)^{-1/2} \\ C_g &= \frac{1}{U}\frac{d\omega}{dk} = \frac{C}{2}\left(1+\frac{\kappa H e^{-\kappa H}}{\sinh(\kappa H)}\right) \end{aligned} \ . \tag{9}$$

The hydrodynamic crest pattern for H = 0.1 is shown in Figure 2; the source is moving to the left and only one half of the pattern is plotted. Each crest terminates at the source. However, it should be noted that interpretation of radar wakes depends on the radar controlling variable (e.g. surface velocity) and observed patterns can be shifted in phase [5], depending on the method of observation [6]. The axes are expressed in normalized Cartesian (x, y) coordinates and the first five crests are depicted. The outer crest is a straight line, which represents a caustic produced when a group of waves coalesce as in a Mach cone. Otherwise the shape of each crest line is the same; they differ only by an integer scale factor. The distance between successive crests appears to decrease as the center of the wake is approached. Figure 3 shows the pattern for H = 0.001. As H decreases, the crests move closer together and, as expected, the maximum wake angle decreases according to (8).

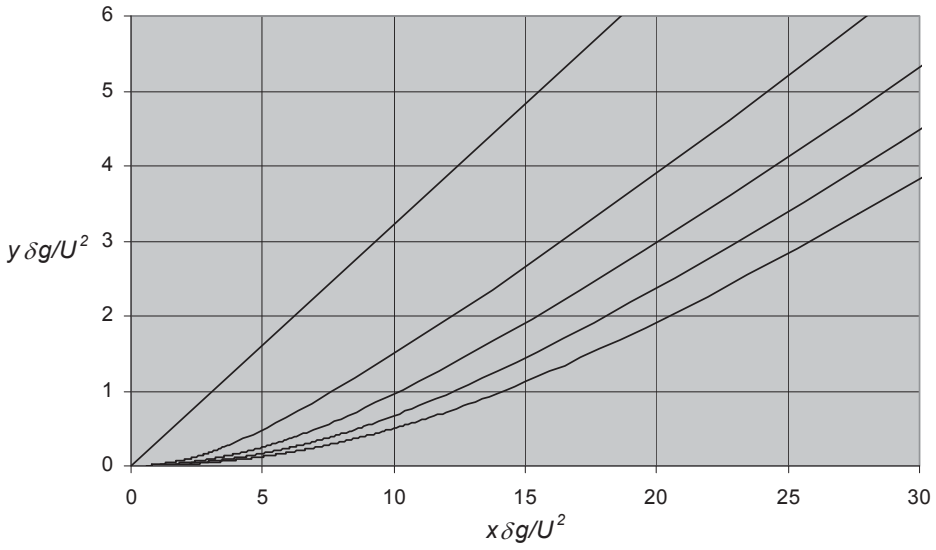

Figure 2: Crest pattern on a discrete interface for H = 0.1.

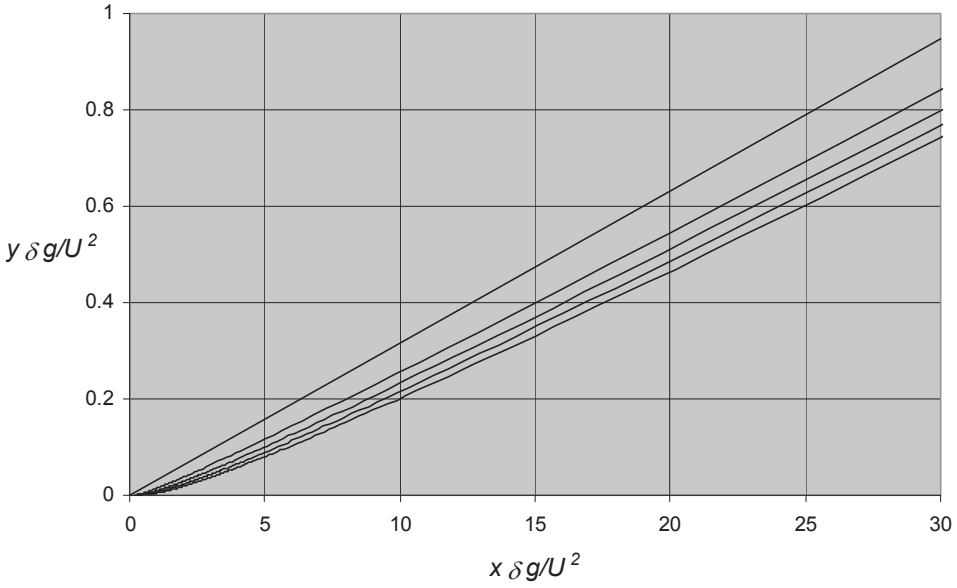

Figure 3: Crest pattern on a discrete interface for H = 0.001.

The amplitudes of internal waves in a wake on a discrete interface were considered by Hudimac [16]. As noted above, he also found that when the source moves at speeds less than the maximum wave speed, both divergent and transverse waves are created. However the theory did not predict

that these two wave systems should meet at the wake edge, which is a caustic, as in the Kelvin wake. Therefore the theory is deficient. The problem was revisited in the 1990s (e.g. [36]) and it was recognized that the poles in a double integral just correspond to the allowed waves (as described in Annex D and which were calculated using this approach); the approach was also generalized to include unsteady wakes [38].

2.3 Waves on a diffuse interface

In most cases the internal layer is diffuse and is described by the B-V frequency, N. This is defined in terms of the slope of the water density in the vertical, z-direction (positive upwards), i.e.:

$$N^2(z) = -\frac{g}{\rho(z)}\frac{d\rho(z)}{dz}. \tag{10}$$

For example, Figure 4 shows an example of a B-V frequency profile. This is the type of profile that might be observed in the Straits of Gibraltar [39], but minor variations have been smoothed out; it resembles the profile shown by Lighthill [7] except that there is no mixed region at the surface. The profile has been modeled as a Lorentzian function so that its tails fall off slowly at extreme depth:

$$N(z) = \frac{N_{\max} a^2}{(z-b)^2 + a^2}, \tag{11}$$

where $N_{\max}$ = 0.015 rad/s, a = 100 m and b = 60 m.

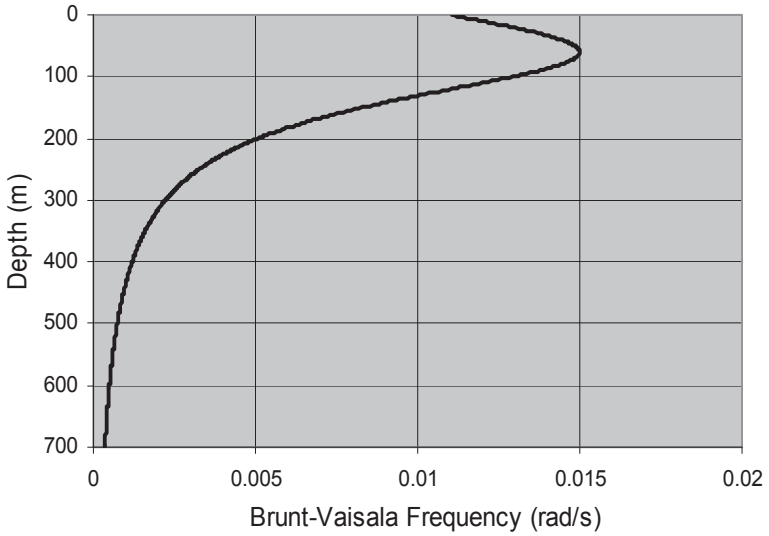

Figure 4: Typical Brunt-Väisälä vertical profile.

We look for horizontal wave-like solutions of the vertical component of fluid mass flux, q:

$$q = Q(z)e^{i(\omega t - ks)}, \tag{12}$$

where ω is the angular frequency of the waves, k is the horizontal wave vector and s is the distance propagated. The equation, which controls internal waves (e.g, [4], [7]), is:

$$\frac{d^2Q}{dz^2} + k^2\left(\frac{N^2}{\omega^2} - 1\right)Q = 0\,. \tag{13}$$

The value of ω can be regarded as given, while k must be determined by boundary conditions (or *vice versa*).

If $N > \omega$, the solution for Q is oscillatory (as a function of z) but otherwise the solutions are exponential and the solution must decrease with distance from the layer. At the surface of the water, the vertical mass flux is assumed to be zero. If (13) is integrated numerically for arbitrary k, the vertical displacement and velocity at the maximum depth are apt to be unbounded, which is clearly unphysical. Therefore values of k must be found that admit reasonable solutions, which are small both at the surface and at the ocean floor.

A Runge-Kutta method of integrating (13) was used to find the appropriate values of horizontal angular wave number k for a sequence of angular frequencies, ω. (An algorithm described in Numerical Recipes [40] was adapted and coded in C#.) The vertical component of fluid velocity

at the surface was set equal to zero and its slope was given a small value. An integration of the differential equation was performed to determine the vertical component of fluid velocity at the ocean bottom. After each integration, the value of k was corrected. The correction used a binary search approach to determine a value of the angular wave number that resulted in a very small value of Q at the ocean bottom.

To solve (13), it was necessary to guess an initial value of k. This was achieved using the Wentzel-Kramers-Brillouin (WKB) approximation [41], [42]. An approximation to the phase over the oscillatory portion of the vertical profile must be roughly equal to $(n + 1)\pi$, where n is the mode number (starting at zero):

$$k \int_{\Delta z} \sqrt{\frac{N^2}{\omega^2} - 1}\, dz \approx (n+1)\, \pi \tag{14}$$

where Δz is the range of integration for which the argument of the square root is positive.

The entire process was not very computationally efficient, but it was very robust and only took a few seconds on a standard PC.

As described in [4] and [7], for each ω, there exists a sequence of solutions corresponding to the sinuous and varicose modes. The zeroth (sinuous) mode has no zero crossings and so represents an up and down motion of the entire layer. The first mode has one zero crossing and corresponds to a varicose mode, and so on.

The result for the profile in Figure 4 is shown in Figure 5. Each of the mode graphs resembles that in Figure 1 in that the phase and group velocities are highest near the origin but, while the frequency in Figure 1 increases without bounds as k increases, the frequency is bounded in Figure 5. Also the phase and group velocities are highest for the lowest mode, which we call the zeroth mode.

In contrast to the discrete interface, the group velocity, which is equal to the slope of the dispersion graph, rapidly approaches zero at large values of angular wave number; as expected, the maximum angular frequency of propagating waves is equal to the B-V frequency. This suggests that the very short wavelength waves, which comprise the divergent system that propagates almost perpendicularly to the source track, are suppressed.

For this particular example, the phase and group velocities in the zeroth mode at small angular wave number are about 1.19 m/s. It is interesting to compare this value with the discrete model. This can be accomplished from the definition of the B-V frequency (10), which gives:

$$N_{\max}^2 \approx \frac{g\delta}{\Delta}, \tag{15}$$

where Δ is the layer width. We can combine this with an expression for the maximum wave velocity, which can be derived from (5):

$$c_{\max} = \sqrt{\delta g h} = N_{\max} \sqrt{h\Delta} \tag{16}$$

The depth and width of the layer are both about 100 m and the peak B-V frequency is 0.015 rad/s. This gives a maximum wave velocity of about 1.5 m/s, which is comparable to that obtained by an exact analysis.

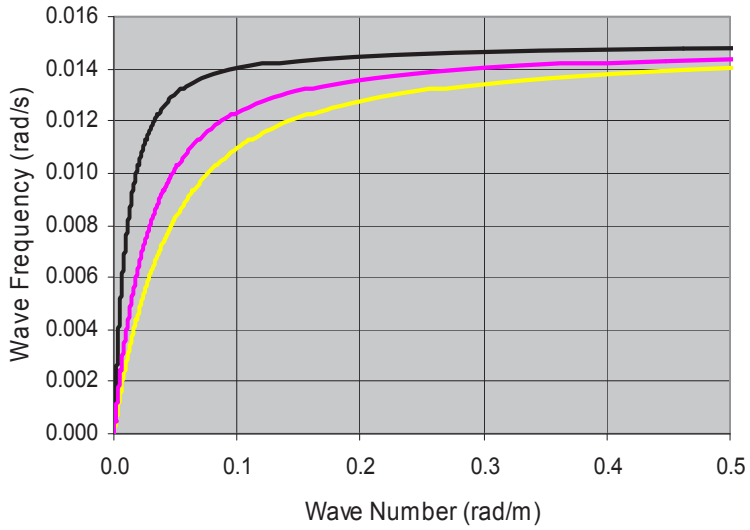

Figure 5: Dispersion relation for three modes: zeroth (—); first (—) second (—).

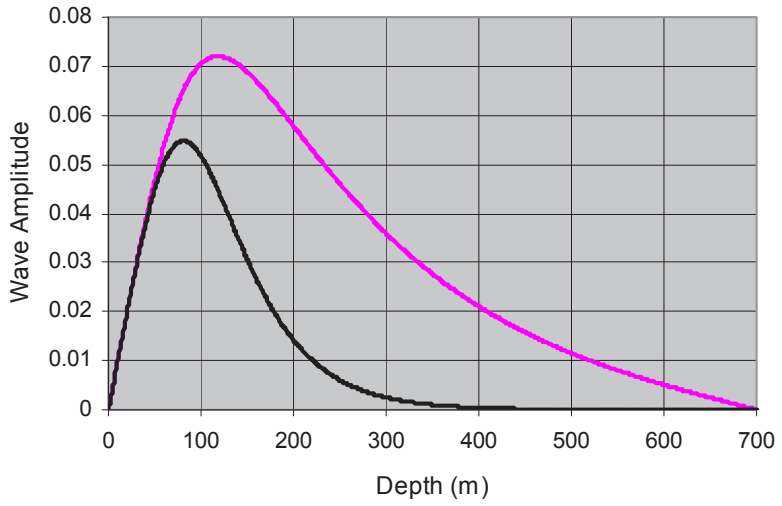

Figure 6: Eigenfunctions for the zeroth mode: ω = 0.005 rad/s (—); ω = 0.01 rad/s (—).

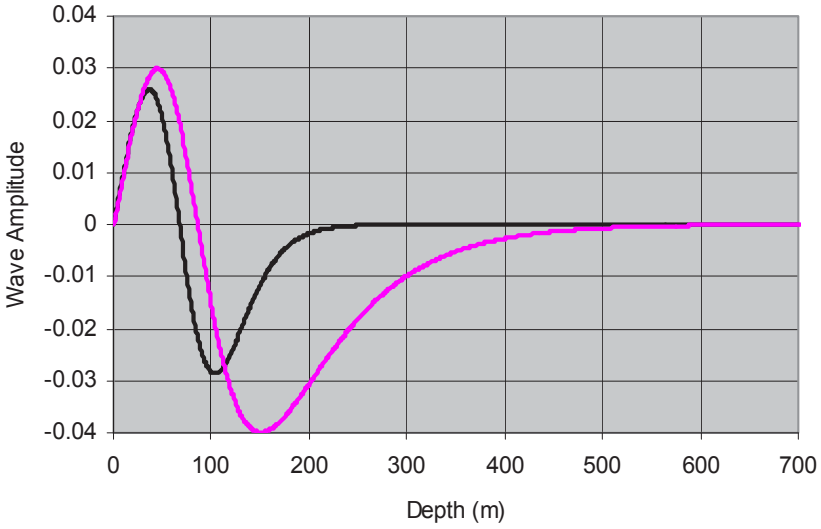

Figure 7: Eigenfunctions for the first mode: ω = 0.005 rad/s (—); ω = 0.01 rad/s (—).

Figure 6 shows eigenfunctions for the differential equation (13). This is for the zeroth mode at two different angular frequencies, namely 0.005 rad/s and 0.01 rad/s. The amplitudes are not normalized and were calculated assuming the slope of the eigenfunction at the origin is 0.001 m^{-1}. As can be seen, the zeroth mode has no zero crossing while the first mode in Figure 7 has just a single crossing; this latter clearly represents a varicose mode.

The differential equation happens to be an example of the Sturm-Liouville equation with the condition that the solutions vanish at the boundaries. Therefore the eigenfunctions can be made to form an orthonormal set [42] such that:

$$\int Q_i(z) Q_j(z) \left(\frac{N(z)^2}{\omega^2} - 1 \right) dz = \delta_{ij} \tag{17}$$

It has been verified that this is indeed valid (for example with the data in Figure 6 and Figure 7). Orthonormality implies that a source function can be expanded in terms of eigenfunctions. This opens a path to calculating the wake amplitudes.

The other potentially useful attribute of the crest pattern is its angular width. This is related to the maximum group velocity, which is stated above and is about 1.19 m/s. When the source moves at a speed of 5 m/s, this gives a maximum wake half angle of about 13.8º. (The crest pattern is independent of the source depth.) Figure 8 shows the crest pattern for the zeroth mode, which confirms this. A notable feature of the pattern is the rearward offset of each crest in the *x*-direction. This results in each crest terminating in a cusp; this type of pattern was observed during the Loch Linnhe trials [6].

The pattern for the first mode is depicted in Figure 9. As expected from the dispersion relation in Figure 5, the crest pattern has a smaller opening angle because the group velocity near the origin is smaller than in the zeroth mode. It is probably unnecessary to consider more modes because it is unlikely that they will be excited to any significant extent, as will be discussed later.

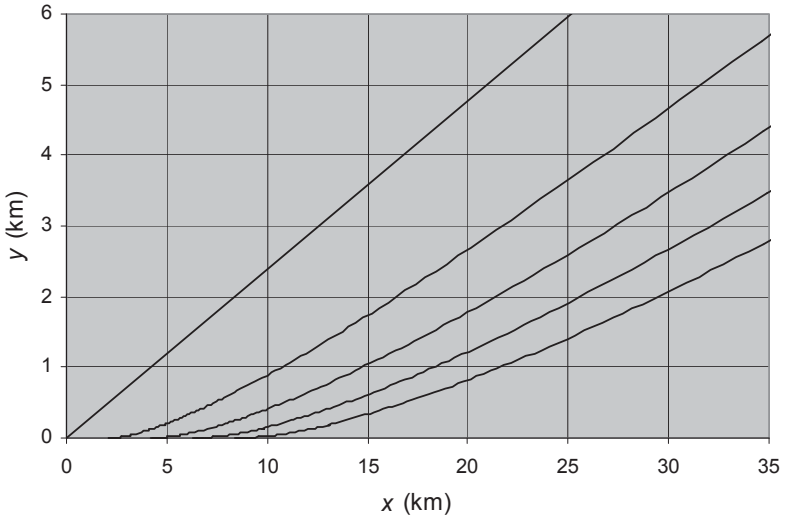

Figure 8: Zeroth mode crest pattern for a source moving horizontally at 5 m/s in the profile of Figure 4.

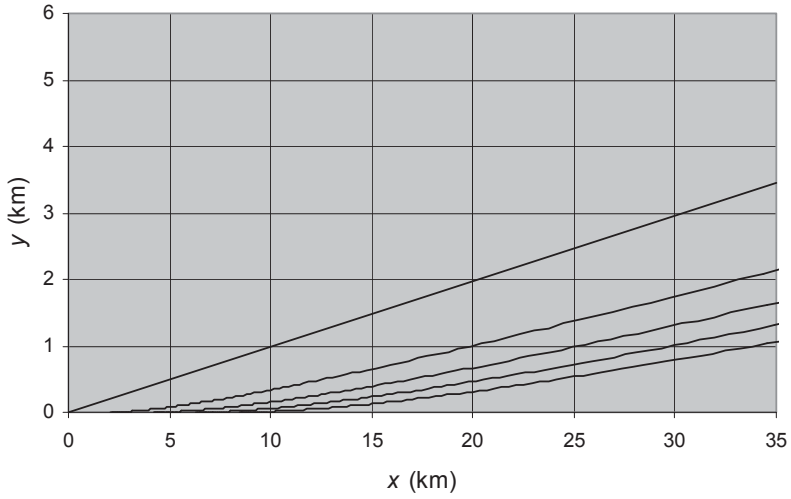

Figure 9: First mode crest pattern for a source moving horizontally at 5 m/s in the profile of Figure 4.

The cusps are separated by a fixed distance. This has been examined in [20] where it is shown that the separation distance, d, is given by:

$$d = \frac{2\pi U}{N_{\max}}. \tag{18}$$

In the examples above, U = 5 m/s and $N_{\max}$ is 0.015 rad/s. Therefore we have d = 2094.4 m. This is consistent with the crests in Figure 8 and Figure 9. In contrast, when the layer can be modeled as a discrete interface, all crests intersect the origin.

3 Loch Linnhe trials

The Loch Linnhe trials were conducted from 1989 to 1994 specifically to study the generation of internal wave wakes from moving surface ships. Some of the experimental conditions for experiments from 1991 to 1994 are described by Mullenhoff and Brase [43]. Ship displacements ranged from 100 tons to 10,000 tons and data were acquired for various wind speeds up to 15 m/s. The peak B-V frequencies were quite high ranging from 0.02 rad/s to 0.17 rad/s, while the associated depths ranged from 1 m to 17 m. The ship speeds ranged from 1 m/s to 4 m/s.

Stapleton and Perry [44] and Stapleton [45] have presented images of ship wakes from the trials. Images of the observed internal wave wake crest patterns are consistent with the diffuse layer theory. In [44], an attempt was made to explain the observed amplitudes in terms of a simple radar scattering model, but this was not very successful. In [45], the emphasis is on a comparison between internal wave wakes and narrow-V wakes, which were also observed in the trials.

Watson et al. [47] also present some excellent images of internal wave wakes. They describe the B-V profile of the loch, as shown in Figure 10 (extracted from data in the paper). This shows that the layer was concentrated over a narrow depth range, but its smoothed shape is similar to that used in our example in a previous section.

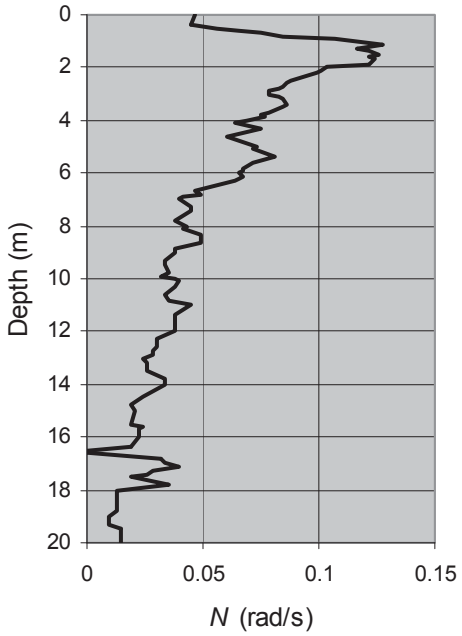

Figure 10: B-V Frequency profile.

The method used to derive the crest pattern appears to be similar to that used here, but no details are provided. However, it is claimed that the crest patterns derived from the B-V data were in

satisfactory agreement with the observations. An attempt was made to estimate wave amplitudes but again it is not clear that this was successful.

In a later paper, Hogan et al. [6], analyzed Loch Linnhe imagery and showed unequivocally that the theory of wake crests on a diffuse layer agrees very well with their observations. Their summary includes an excellent description of the imaging mechanism involving Bragg scattering but this is not pursued and the authors note some problems with Bragg wave relaxation rates, especially at the higher radar frequencies (K_u-band); the treatment is qualitative.

4 Discussion

During the Loch Linnhe trials, which involved some moderately large surface ships, Hogan et al. [6] observed some clear internal wave wakes. The crest patterns derived from theory agreed very well with the observations. In particular, the crest patterns exhibited a rearward offset between each crest, which characterizes diffuse layers. This was observed though the layer was quite thin and it might reasonably have been supposed that it approximated a discrete layer. This shows that the finite thickness of the layer is important, even in these conditions.

The Keller and Munk [20] theory seems to be adequate to explain the crest patterns of internal waves in both discrete and diffuse internal layers. Some authors have attempted to derive surface flow amplitudes, though no details are provided. The estimates probably provide an order of magnitude match to the observations. One approach used the thin ship model of sources and sinks on the ship center-plane. Therefore it is reasonable to suppose that an adequate theoretical background exists to model surface flows from both surface and sub-surface ships.

The derivation of the far wake crest pattern involves the calculation of an angular wave vector at each point in the wake. This value represents the propagation of the surface wave field at that point and takes into account the Doppler relation and the dispersion characteristics of the medium. It turns out that the value of the wave vector only depends on the angle between a vector, which joins the source (at the wake apex) to the point in the wake, and the ship's track. Therefore it is only necessary to perform a limited number of calculations to determine the values over the entire wake. Simulation of the wake crest pattern is greatly simplified. Moreover the wave vector can be regarded as a parameter that varies continuously along a wake crest for which the phase is constant. For example, for a divergent wave pattern, the wave number is large near the wake apex and decreases monotonically; it approaches zero as the crest approaches the wake edge. This explains in part why the crest offset is determined by the peak B-V frequency.

Simulation of the far wake can be treated as an eigenvalue problem, which is relevant not only to the crest pattern but also to the estimation of the wave amplitudes in the wake. Technically, a pole appears in an integral for the amplitude so that the integrand peaks sharply at this eigenvalue. This allows the integral to be evaluated quite accurately except near the wake edge. (Near the caustic, special techniques can be employed but this is beyond the scope of the report.) For the discrete interface, the same methodology applies but the eigenvalues are solutions of the dispersion relation with ω replaced by $\mathbf{k.U}$.

Measurements of the surface flow velocities, which are responsible for the SAR imaging of the wakes, were less than about 2 cm/s. Such velocities are a small but significant fraction of the group velocity of Bragg waves associated with the SARs, which operate at L, C and X and other microwave bands. The literature strongly suggests that the primary mechanism for imaging internal wave wakes and possibly other oceanic features and ship wake components is through a modulation of the Bragg waves by variations in the surface flow field. There are a number of simplified theoretical approaches but it is not clear that they are satisfactory.

Scattering models have been described by a number of authors, such as Alpers [8], Hughes [48] and others in [49] to [51]. The problem is that the simple approaches to radar scattering tend to be based on linear theory whereas a consideration of wave propagation in such a flow field suggests

that non-linear effects can play a significant role. This can be appreciated by considering a simple ray model in which the rays impinge on a weak flow at a narrow angle and are reflected; in linear theory they continue in a straight line. A careful evaluation of backscattering models would be useful and could indicate the range of validity of the models and their utility in describing wakes.

A vessel traveling well above or well below an internal layer can only excite sinuous waves; these correspond to our mode zero and other even integer modes. Varicose modes cannot be excited effectively. When the excitation is partly in the layer, the main excitation will generally be in the zeroth mode with some in odd and even modes corresponding to varicose and other hybrid oscillations. However, when the source function results in smoothly varying excitations over depth, it is difficult to understand how high order modes can be excited effectively. Therefore it is likely that only the zeroth sinuous mode and possibly the first varicose mode are important.

5 Conclusions

The successful simulation of internal wave wake crest patterns has been described in previous literature for internal layer models over a range of complexity, from the simple discrete interface to more complicated, realistic B-V profiles. However, previous authors have omitted some essential details. Also the simulation of horizontal surface velocity amplitudes has been attempted, but apparently with limited success. In the case of flow amplitudes, little information on the methodology has been published. The literature indicates that existing theory is probably capable of predicting the horizontal surface flow velocities more or less correctly.

This report provides details on the derivation of crest patterns for the discrete internal interface and for the diffuse layer. In Annex E it also describes a methodology for calculating the surface velocity amplitudes from a source (or a distribution of sources by linear combination).

The remainder of the problem concerns the effect of the surface velocities on the radar scattering. This still seems to require some effort because it appears that non-linear effects are important. A previous approach to this problem was described by Tunaley [9], who employed simple ray-tracing to determine the amplitudes of the Bragg waves at a point in the wake by relating them to waves generated outside of it. This included refraction of the waves in the flow field and the exchange of energy between the waves and the flow field through conservation of wave action. However, the relaxation of the Bragg waves due to viscosity and other mechanisms was largely neglected.

Another area of importance in modeling internal wave wakes is the detail of the ship representation. This should include the collapsing turbulent wake, which still seems to be an area of research. However, to establish the detectability of surface and sub-surface vessels, a simple model may be sufficient. This could be a single source of appropriate strength or the thin-ship model similar to [21]. More complicated panel models are another possibility; these are not particularly difficult to apply.

The mechanisms that are responsible for the wake of a surface ship are equally applicable to a submarine. The treatment here has focused on internal waves as trapped waveguide modes traveling horizontally but this is not the only representation; they also propagate in a vertical direction. Therefore an internal layer can effectively transmit a disturbance from the depths to the surface. The observation of surface ship wakes in the Loch Linnhe trials strongly suggests that a submarine traveling at a depth of several tens of meters under similar conditions would be detectable. However, the existence of a surface mixed layer would tend to suppress any disturbance at the surface, especially if the mixed layer were thick. Therefore it is reasonable to conclude that submarines are only detectable under appropriate conditions. These include the existence of a suitably strong layer over a wide depth range and the absence of a thick mixed layer near the surface.

The report has not discussed the reflection of ambient internal waves by a vessel. These could be important because they could be Doppler shifted into a frequency range of importance for detectability and gain energy from the vessel during the reflection process.

Definite conclusions must await a full simulation including surface flow amplitudes.

References

[1] D.M. Roy, Oceanographic and Atmospheric Effects on RADARSAT-2 Imagery of Ship Wakes, MSc Thesis, Royal Military College, Kingston ON, August 2009.

[2] D.M. Roy and J.K.E. Tunaley, Visibility of Turbulent Ship Wakes in Dual-Polarized RADARSAT-2 Imagery, London Research and Development report, March 2010, http://www.london-research-and-development.com.

[3] I. Hennings, R. Romeiser, W. Alpers and A. Viola, Radar Imaging of Kelvin Arms of Ship Wakes, *Int. J. Remote Sensing*, Vol. 20, No. 13, pp 2519-2543, 1999.

[4] O.M. Phillips, *The Dynamics of the Upper Ocean*, 2nd Ed., Cambridge University Press, New York, 1977.

[5] X. Li, J. Morrison, L. Pietratesa and A. Ochadlick, Analysis of Oceanic Internal Waves from Airborne SAR Images, *J. Coastal Research*, Vol. 15, No. 4, pp 884-891, 1999.

[6] G.G. Hogan, R.D. Chapman, G. Watson and D.R. Thompson, Observations of Ship-Generated Internal Waves in SAR Images of Loch Linnhe, Scotland, and Comparison with Theory and in situ Internal Wave Measurements, *IEEE Trans. Geosci. Remote Sens.*, Vol. 34, No. 2, pp 532-542, March 1996.

[7] J. Lighthill, *Waves in Fluids*, Cambridge University Press, 1980.

[8] W. Alpers, Theory of Radar Imaging of Internal Waves, *Nature*, Vol. 314, pp 245-247, 1985.

[9] J.K.E. Tunaley, Further Modifications to the DREO Ship Wake Algorithms, London Research and Development Corp. final report under contract W7714-6-0014/01-SV, January 1997.

[10] D.E. Mowbray and B.S.H. Rarity, A Theoretical and Experimental Investigation of the Phase Configuration of Internal Waves of Small Amplitude in a Density Stratified Liquid, *J. Fluid Mech*., Vol. 28, No. 1, pp 1-16, 1967.

[11] B.S.H. Rarity, The Two-Dimensional Wave Pattern produced by a Disturbance Moving in an Arbitrary Direction in a Density Stratified Liquid, *J. Fluid Mech*., Vol. 30, Part 2, pp 329-336, 1967.

[12] D.E. Mowbray and B.S.H. Rarity, The Internal Wave Pattern Produced by a Sphere in a Density Stratified Medium , *J. Fluid Mech*., Vol. 30, No. 3, pp 489-495, 1967.

[13] T.N. Stevenson, Some Two-Dimensional Internal Waves in a Stratified Fluid, *J. Fluid Mech*, Vol. 33, No. 4, pp 715-720, 1968.

[14] T.H. Havelock, Ship Waves: The Relative Efficiency of Bow and Stern, *Proc. Roy. Soc. Lond. A*, Vol. 149, pp 417-426, 1935.

[15] W. Qui, A Panel-Free Method for Time Domain Analysis of Floating Bodies in Waves, PhD Thesis, Dalhousie University, Halifax NS, June 2001.

[16] A.A. Hudimac, Ship Waves in a Stratified Ocean, *J. Fluid Mech.*, Vol. 11, pp 229-243, 1961.

[17] J.W. Miles, Internal Waves, Generated by a Horizontally Moving Source, *Geoph. Fluid Dyn*., Vol. 2, pp 63-87, 1971.

[18] V.A. Borovikov, V.V. Bulatov and Y.V. Vladimirov, Internal Gravity Waves Excited by a Body Moving in a Stratified Fluid, *Fluid Dynamics Res.*, Vol. 15, pp 325-336, 1995.

[19] V. Borovikov, V. Bulatov, M. Gilman and Y. Vladimirov, Internal Gravity Waves Excited by a Body Moving in a Stratified Fluid, *Proc. 22nd Symposium on Naval Hydrodynamics*, Washington DC, August 1998.

[20] J.B. Keller and W.H. Munk, Internal Wave Wakes of a Body Moving in a Stratified Medium, *Physics of Fluids*, Vol. 13, No. 6, pp 1425-1431, 1970.

[21] K.B. Dysthe and J. Trulsen, Internal Waves from Moving Point Sources, *John Hopkins APL Technical Digest*, Vol. 10, No. 4, pp 307-316, 1989.

[22] A.H. Schooley and R.W. Stewart, Experiments with a Self-Propelled Body Submerged in a Fluid with a Vertical Density Gradient, *J. Fluid Mech*., Vol. 15, No., pp 83, 1963.

[23] J. Wu, Mixed Region Collapse with Internal Wave Generation in a Density-Stratified Medium, *J. Fluid Mech*., Vol. 35, Part 3, pp 591, 1969.

[24] A.H. Schooley and B.A. Hughes, An Experimental and Theoretical Study of Internal Waves Generated by the Collapse of a Two-Dimensional Mixed Region in a Density Gradient, *J. Fluid Mech., Vol.* 51, pp 159-174, 1972.

[25] T.W. Kao, Principal Stage of Wake Collapse in a Stratified Fluid: Two-Dimensional Theory, *Physics of Fluids*, Vol. 19, No. 8, pp 1071-1074, August 1976.

[26] R. J. Hartman and H. W. Lewis, Wake Collapse in a Stratified Fluid: Linear Treatment, *J. Fluid Mech.,* 51, Part 3, pp 613-618, 1972.

[27] T.N. Stevenson, Some Two-dimensional Internal Waves in a Stratified Fluid, *J. Fluid Mech*., Vol. 33, Part 4, pp 715-720, 1968.

[28] T.N. Stevenson, Asymmetrical Internal Waves Generated by a Travelling Oscillating Body, *J. Fluid Mech*., Vol. 35, Part 2, pp 219-224, 1969.

[29] T.N. Stevenson and N.H. Thomas, Two-Dimensional Internal Waves Generated by a Traveling Oscillating Cylinder, *J. Fluid Mech*., Vol. 36, Part 3, pp 505-511, 1969.

[30] T. H. Bell, Jr. and J.P. Dugan, Model for Mixed Region Collapse in a Stratified Fluid, *J. Eng. Math*., Vol. 8, No. 3, pp 241-248, July 1974.

[31] R.G. Rehm and H.S. Radt, Internal Waves Generated by a Translating Oscillating Body, *J. Fluid Mech*., Vol. 68, Part 2, pp 235-258, 1975.

[32] J.-T. Lin and Y.-H. Pao, Wakes in Stratified Fluids, *Ann. Rev. Flu Mech. 11* 317-338, 1979.

[33] B. Voisin, Internal Wave Generation in Uniformly Stratified Fluids. Part 1. Green's Function and Point Sources, *J. Fluid Mech*., Vol. 231, pp 439-480, 1991.

[34] G.R. Spedding, The evolution of initially turbulent bluff-body wakes at high internal Froude number, *J. Fluid Mech*. Vol. 337, pp 283-301, 1997.

[35] H.F. Robey, The Generation of Internal Waves by a Towed Sphere and Its Wake in a Thermocline, *Physics Fluids*, Vol. 9, No. 11, pp 3353-3367, 1997.

[36] M. Bonnier and O. Eiff, Experimental Investigation of the Collapse of a Turbulent Wake in a Stably Stratified Fluid, *Physics Fluids*, Vol. 14, No. 2, pp 791-801, February 2002.

[37] J.K.E. Tunaley, Algorithms for the Simulation of a SAR Image of a Surface Ship Wake, London Research and Development Report for DRDC Ottawa under contract 007SV.W7714-3-9775, February 1995.

[38] J.K.E. Tunaley, The Unsteady Wake from a Body Moving Near an Internal Layer, Proc. 5th Canadian Conference on Marine Hydrodynamics, St. Johns, Newfoundland, pp 5-13, 1999. Updated at http://www.london-research-and-development.com/Internal Wakes.Version2.pdf.

[39] J.R. Apel, Oceanic Internal Waves and Solitons, in *An Atlas of Oceanic Internal Solitary Waves*, Global Ocean Associates Report for the Office of Naval Research Code 322 PO, 2002. (http://www.internalwaveatlas.com/Atlas_index.html)

[40] W.H. Press, B.P. Flannery, S.A. Teukolsky and W.T. Vetterling, *Numerical Recipes*, Cambridge University Press, New York, 1986.

[41] J. Matthews and R.L. Walker, *Mathematical Methods of Physics*, 2nd Ed., Benjamin, New York, 1970.

[42] R. Courant and D. Hilbert, *Methods of Mathematical Physics*, Vol. I, John Wiley, New York, 1953.

[43] C.J. Mullenhoff and J.M. Brase, A Qualitative Study of Internal Wave Ship Wakes: Dependence on Environmental Conditions and Experimental Parameters, Lawrence Livermore National Laboratories, Contract report for US Department of Energy W-7405-Eng-48, April 1995.(http://www.osti.gov/bridge/servlets/purl/86885-LQrl1l/webviewable/86885.pdf)

[44] N.R. Stapleton and J.R. Perry, Synthetic Aperture Radar Imaging of Ship Generated Internal Waves During the UK/US Loch Linnhe Series of Experiments, *Proc.IGARSS '92, International Remote Sensing Symposiu*m, *Houston, Texas*, Vol. 2, pp 1338-1340, 1992.

[45] N.R. Stapleton, Ship Wakes in Radar Imagery, *Int. J. Remote Sens*., Vol. 18, No. 6, pp 1381-1386, 1997.

[46] N.R. Stapleton, Backscatter Modelling of Ship-Generated Internal Wave Wakes Observed During the Loch Linnhe Series of Experiments, *Proc. IGARSS '94*, *International Remote Sensing Symposiu*m, *Pasedena, California*, Vol. 2, pp 1732-1734, 1994.

[47] G. Watson, R. Chapman and J. Apel, Measurements of the Internal Wave Wake of a Ship in a Highly Stratified Sea Loch, *J. Geophys. Res*., Vol. 97, No. C6, pp 9689-9703, June 1992.

[48] B.A. Hughes, The Effect of Internal Waves on Surface Wind Waves 2. Theoretical Analysis, *J. Geophys. Res*., Vol. 83, No. C1, pp 455-465, 1978.

[49] D.R. Thompson and R.F. Gasparovic, Intensity Modulation of Internal Waves, *Nature*, Vol. 320, pp 345-348, March 1986.

[50] K. Ouchi, On the SAR Imaging Mechanisms of Oceanic Waves*, Proc. IGARSS '93*, *International Remote Sensing Symposiu*m, *Tokyo, Japan*, Vol. 2, pp 357-360, 1993

[51] K. Ouchi, N.R. Stapleton and B.C. Barber, Multi-Frequency SAR Images of Ship Generated Internal Waves, *Int. J. Remote Sens*., Vol. 18, No. 8, pp 3709-3718, 1997.

[52] N.W. MacLachlan, *Bessel Functions for Engineers*, Oxford Clarendon Press, 1961.

Annex A The source in the frequency domain

The first step is to establish the velocity potential for a source of fluid fixed in position at (a, b, c). This relies on the identity:

$$\begin{aligned}\frac{1}{r} &= \frac{1}{\sqrt{(x-a)^2+(y-b)^2+(z-c)^2}} \\ &= \frac{1}{2\pi}\int_{-\pi}^{\pi}\int_{0}^{\infty} e^{-k|z-c|}e^{-ik((x-a)\cos\theta+(y-b)\sin\theta)}\,d\theta\,dk\end{aligned}. \tag{A.1}$$

A unit source located in an infinite body of water gives rise to a velocity potential:

$$\Phi = -\frac{1}{4\pi r}. \tag{A.2}$$

In the following z is positive upwards. Equation (A.1) resembles a two-dimensional Fourier transform so that, assuming a time-frequency dependence, $e^{i\omega t}$, the effect of a velocity potential perturbation can be found easily in the spatial frequency domain.

The result can be derived by first integrating (A.1) with respect to θ. Simplifying by setting $a = b = 0$, this gives:

$$\int_{0}^{\infty} e^{-k|z-c|}J_0(kr)dk = \frac{1}{r}. \tag{A.3}$$

The integral is a standard result [52].

Annex B Derivation of the crest pattern

We are concerned with the crest pattern in the far wake because this is dominated by dispersive effects and can be described in terms of the phase and group velocities of the waves. The geometry is shown in Figure B-1. The ship, S, which is moving to the left, creates a perturbation in the fluid at points along its track. The perturbation is stationary in the reference frame of the ship so that its phase is constant and can be set to zero. A wave created at O will propagate a distance, s, determined by the group velocity and the elapsed time, τ. The other constraint involves the Doppler equation. According to (1), this leads to a condition on the phase velocity, c:

$$\omega / k = c = U \cos\theta , \tag{B.1}$$

where θ is the angle between the wave vector and the ship's track.

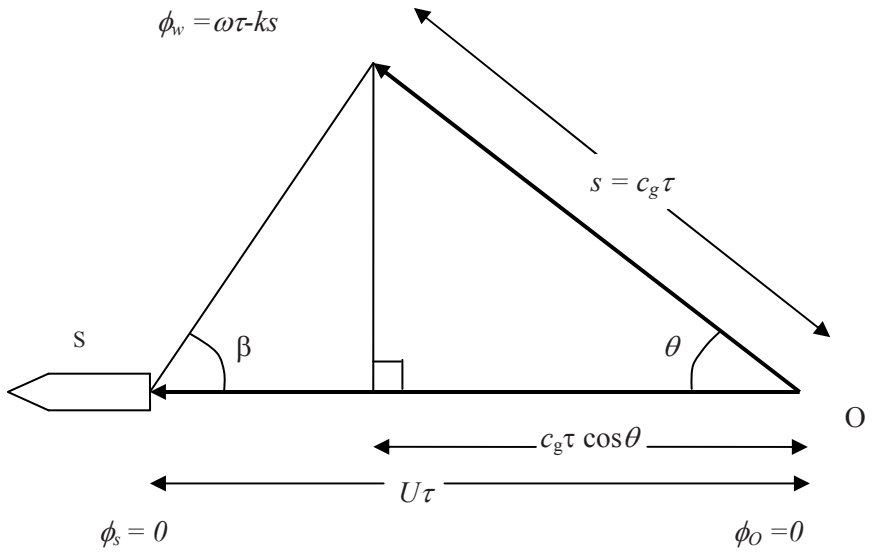

Figure B-1: The geometry of the crest pattern.

From the geometry the positions of crests may be found readily in the following way. If the origin is at S, and the x-axis lies along SO, we have:

$$\begin{aligned} x &= (U - c_g \cos\theta)\tau = (U - cc_g / U)\tau \\ y &= c_g \tau \sin\theta = c_g \tau \sqrt{1 - \frac{c^2}{U^2}} \end{aligned} \quad , \tag{B.2}$$

where c_g is the group velocity equal to $d\omega/dk$. Both the phase and group velocities are functions only of k. The propagation time for a crest can be determined by setting the phase to an integer multiple of 2π, i.e.

$$2\pi n = \omega\tau - ks = k(c - c_g)\tau \,. \tag{B.3}$$

The integer n can be interpreted as a crest number, which is zero for the caustic, one for the next crest on the wake interior and so on. Now, if we specify k and n, we can calculate τ from (B.3) because the phase and group velocities can be found from the dispersion relation. Then the values can be entered into (B.2) to find the position (x, y). Therefore k can be regarded as a parameter that varies along a crest. Because the variables x, y and τ are all proportional to n, it follows that all crests have the same shape and are just scaled by n.

Alternatively, it is possible to specify a position (x, y) in the wake and find a value for k and the phase. This is achieved by eliminating τ from (B.2) and (B.3) to yield:

$$\tan\beta = \frac{y}{x} = \frac{c_g\sqrt{1 - c^2/U^2}}{U(1 - cc_g/U^2)} \,. \tag{B.4}$$

The right hand side is just a function of k and the equation can be inverted to yield its value as a function of β. Then τ can be found from one of the equations in (B.2) and inserted into (B.3) to find the phase.

This procedure yields the crest pattern for the Kelvin wake generated by a point source. A simulation of the Kelvin wake amplitudes (not described here), which displays the pattern, is shown in Figure B-2.

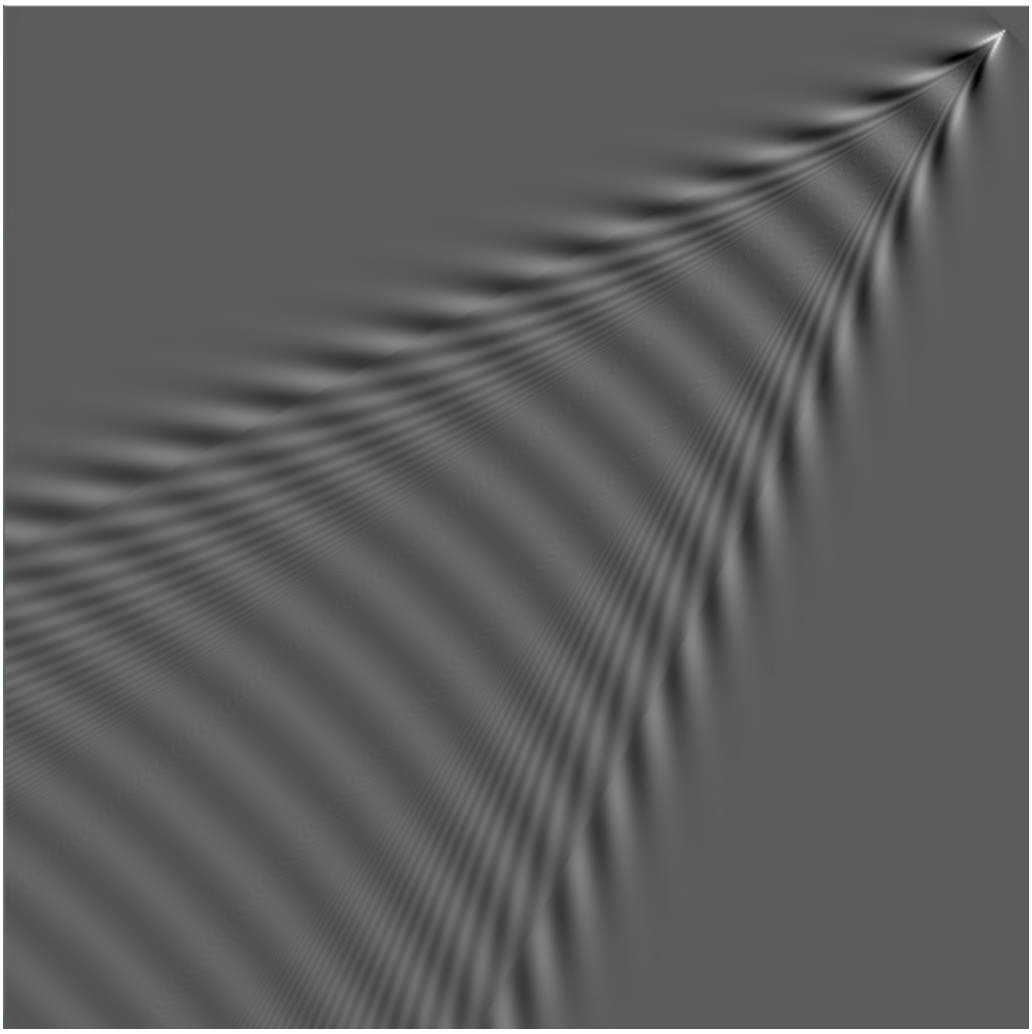

Figure B-2: The Kelvin wake crest pattern.

Annex C Dispersion due to a discrete interface

Fluid of density ρ_1 lies over heavier fluid of density ρ_2 to provide a discrete interface at depth h. The vertical coordinate, z, is measured from the fluid surface and is positive upwards. It is assumed that the fluid is incompressible and inviscid and that surface waves are entirely decoupled from the internal waves. Moreover, it is assumed that the internal waves do not affect the surface height. Therefore the vertical component of velocity at the surface is zero. The problem can be treated in terms of the velocity potential, Φ:

$$\mathbf{u} = \nabla\Phi\,, \tag{C.1}$$

where $\mathbf{u}$ is the velocity. Because the fluid is incompressible, $\nabla\cdot\mathbf{u} = 0$, so that the velocity potential satisfies Laplace's equation. Assuming that appropriate solutions are oscillatory in the horizontal plane (of the form $\exp(i(\omega t - \mathbf{k}\cdot\mathbf{r}))$ and taking into account the boundary condition at the surface, it is straightforward to show that:

$$\begin{aligned}\Phi_1 &= A(e^{kz} + e^{-kz})\\ \Phi_2 &= Be^{kz}\end{aligned}\,, \tag{C.2}$$

where $\Phi_{1,2}$ are the potentials in the upper and lower fluids and z is positive upwards. The coefficients A and B are functions of the horizontal angular wave vector, $\mathbf{k}$, and the form of the second equation is chosen so that the potential decreases with increasing depth.

There are two boundary conditions at the interface. Firstly the vertical velocity of the fluids on each side of the boundary are the same and are related to the displacement, ζ, of the boundary itself:

$$\left(\frac{\partial\Phi_1}{\partial z}\right)_{z=h} = \left(\frac{\partial\Phi_2}{\partial z}\right)_{z=h} = \frac{\partial\zeta}{\partial t}\,. \tag{C.3}$$

Secondly a consideration of the excess pressure at the unperturbed boundary during a small displacement leads to [4]:

$$\rho_2\frac{\partial\Phi_2}{\partial t} - \rho_1\frac{\partial\Phi_1}{\partial t} + (\rho_2 - \rho_1)g\zeta = 0\,. \tag{C.4}$$

Solving (C.2), (C.3) and (C.4) yields the dispersion equation:

$$\omega^2 = \frac{(\rho_2 - \rho_1)gk}{\rho_2 - \rho_1 \coth(hk)}. \tag{C.5}$$

However, h is negative so that it is often better to write this as:

$$\omega^2 = \frac{(\rho_2 - \rho_1)gk}{\rho_2 + \rho_1 \coth(|\, h \,|\, k)}. \tag{C.6}$$

Annex D Discrete interface amplitudes

The amplitudes on the discrete interface can be calculated in terms of the velocity potential. The disturbance is regarded as a perturbation. The boundary conditions at the surface and the interface are as before but the cases of the source above and below the interface must be treated separately. In the frequency domain we have for a unit source located above the interface:

$$\begin{aligned} \Phi_1 &= Ae^{kz} + Be^{-kz} - e^{-k|z-c|}/(4\pi) \\ \Phi_2 &= Ce^{kz} \end{aligned} . \tag{D.1}$$

Noting that c and h are both negative, we have:

$$\left(\frac{\partial \Phi_1}{\partial z}\right)_{z=0} = 0 = k(A-B) + ke^{kc}/(4\pi) . \tag{D.2}$$

For the source located above the interface, the boundary condition in (C.3) gives:

$$i\omega\zeta = kAe^{kh} - kBe^{-kh} - ke^{k(h-c)}/(4\pi) = kCe^{kh} . \tag{D.3}$$

The boundary condition in (C.4) yields:

$$i\omega\rho_2 Ce^{kh} - i\omega\rho_1\left(Ae^{kh} + Be^{-kh} - \frac{e^{k(h-c)}}{4\pi}\right) + (\rho_2 - \rho_1)g\zeta = 0 . \tag{D.4}$$

In contrast, when the source is below the interface, these equations become:

$$\begin{aligned} \Phi_1 &= Ae^{kz} + Be^{-kz} \\ \Phi_2 &= Ce^{kz} - e^{-k|z-c|}/(4\pi) \end{aligned} , \tag{D.5}$$

$$\left(\frac{\partial \Phi_1}{\partial z}\right)_{z=0} = 0 = k(A-B) , \tag{D.6}$$

$$i\omega\zeta = kAe^{kh} - kBe^{-kh} = kCe^{kh} + ke^{-k(h-c)}/(4\pi) \tag{D.7}$$

and

$$i\omega\rho_2\left(Ce^{kh} - \frac{e^{-k(h-c)}}{4\pi}\right) - i\omega\rho_1\left(Ae^{kh} + Be^{-kh}\right) + (\rho_2 - \rho_1)g\zeta = 0\,. \tag{D.8}$$

These equations can be solved for ζ, A, B and C to give the velocity potential for a unit source. The result for the source above the interface and $z > c$ is (neglecting $1/r$ terms):

$$\Phi_1 = \cosh(kz)\times \\ \frac{\omega^2\left(\rho_2\cosh(k(c-h)) + \rho_1\sinh(k(c-h))\right) - gk(\rho_2 - \rho_1)\cosh(k(c-h))}{2\pi D(\omega,k)(\rho_2\sinh(kh) - \rho_1\cosh(kh))} \tag{D.9}$$

and for the source below the interface:

$$\Phi_1 = \frac{\omega^2\rho_2 e^{-k(h-c)}\cosh(kz)}{2\pi D(\omega,k)(\rho_2\sinh(kh) - \rho_1\cosh(kh))}\,, \tag{D.10}$$

where:

$$D = \omega^2 - \frac{(\rho_2 - \rho_1)gk}{\rho_2 - \rho_1\coth(hk)}\,. \tag{D.11}$$

The surface velocity, **v,** created by an oscillating source of unit strength is given by:

$$\mathbf{v} = -\frac{1}{2\pi}\int_{-\pi}^{\pi}\int_{0}^{\infty} i\mathbf{k}\Phi_1(k, z=0)\, e^{i(\omega t - \mathbf{k}\cdot\mathbf{r})}\, d\theta dk\,. \tag{D.12}$$

Annex E Diffuse layer amplitudes

Following Lighthill [7], the linearized equation of motion of a fluid parcel and the continuity equation (simplified using the Boussinesq approximation) are:

$$\begin{aligned} &\frac{\partial}{\partial t}(\rho_0 \mathbf{u}) + \nabla p_e = \rho_e \mathbf{g} \\ &\nabla \cdot (\rho_0 \mathbf{u}) = S(\mathbf{r}, t) \end{aligned}, \tag{E.1}$$

where ρ_0 is the unperturbed density, $\mathbf{u}$ is the fluid velocity, p_e is the excess pressure, $\mathbf{g}$ is the acceleration due to gravity and S is the source distribution, which is a function of position, $\mathbf{r}$, and time, t. Treating the vertical coordinate, z, as positive upwards and letting the mass flux $\mathbf{q} = \rho_0 \mathbf{u}$, these equations can be combined to yield for the z-component of $\mathbf{q}$:

$$\begin{aligned} \nabla^2 \left(\frac{\partial q_z}{\partial t} \right) &= -g \nabla^2 \rho_e - \frac{\partial}{\partial z} \nabla^2 p_e \\ &= -g \nabla^2 \rho_e + g \frac{\partial^2 \rho_e}{\partial z^2} + \frac{\partial^2 S}{\partial t \partial z} \end{aligned}. \tag{E.2}$$

We note that the excess density, ρ_e, can be expressed in terms of the mass flux [7]:

$$g \frac{\partial \rho_e}{\partial t} = N^2 q_z . \tag{E.3}$$

Therefore we have:

$$\nabla^2 \left(\frac{\partial^2 q_z}{\partial t^2} \right) = -N^2 \left(\frac{\partial^2 q_z}{\partial x^2} + \frac{\partial^2 q_z}{\partial y^2} \right) + \frac{\partial^3 S}{\partial t^2 \partial z} . \tag{E.4}$$

We now assume that the vertical component of the mass flux is oscillatory in the horizontal plane, namely:

$$q_z = Q(z) \exp(i(\omega t - k_x x - k_y y)) . \tag{E.5}$$

Then (E.4) becomes:

$$\frac{\partial^2 Q}{\partial z^2} + k^2\left(\frac{N^2}{\omega^2} - 1\right)Q = \frac{\partial \hat{S}(\omega, k, z)}{\partial z}, \tag{E.6}$$

where $\hat{S}$ is the time and 2-D spatial Fourier transform of S. This is an inhomogeneous differential equation. It is solved by first finding the solution to the homogeneous equation obtained when the right hand side is set equal to zero. This results in a sequence of eigenvalues, k_n^2 and orthonormal eigenfunctions, $Q_n(z)$. The solution is [41]:

$$Q(z) = \sum_n \frac{Q_n(z)}{k_n^2 - k^2} \int Q_n(z') \frac{\partial \hat{S}(\omega, k, z')}{\partial z'} \left(\frac{N^2}{\omega^2} - 1\right) dz' . \tag{E.7}$$

If a point source, oscillating with angular frequency ω_0 is located at (0, 0, c) and has strength, S_0, it can be represented by:

$$S = S_0 \delta(x)\delta(y)\delta(z - c)e^{-i\omega_0 t} . \tag{E.8}$$

The transform of S is given by:

$$\hat{S} = S_0 \delta(\omega - \omega_0)\delta(z - c) . \tag{E.9}$$

A more convenient form of the integral in (E.7) is obtained by integrating by parts to avoid the derivative of $\hat{S}$. Combining (E.7) with (E.9) yields:

$$Q(z) = -\sum_n \frac{Q_n(z)\delta(\omega - \omega_0)}{k_n^2 - k^2} S_0 \left(\frac{\partial F_n}{\partial z}\right)_{z=c}, \tag{E.10}$$

where

$$F_n = Q_n(z)\left(\frac{N^2(z)}{\omega^2} - 1\right). \tag{E.11}$$

The result for a fixed oscillating source at depth c is:

$$q_z = -\int \sum_n \frac{Q_n(z)\delta(\omega - \omega_0)}{k_n^2 - k^2} S_0 \left(\frac{\partial F_n}{\partial z}\right)_{z=c} e^{i(\omega t - \mathbf{k}\cdot\mathbf{r})} d\mathbf{k} d\omega . \tag{E.12}$$

This can be evaluated by transforming to polar coordinates in the wave number space. The integrand is dominated by the pole that represents outgoing waves and the eigenvalues and eigenfunctions for each mode can be determined numerically from the homogeneous equation with $\omega = \omega_0$.

When the source is moving horizontally, the waves are Doppler shifted from zero frequency in the ocean frame. From the Doppler equation or otherwise, the frequency is given by:

$$\omega_0 = kU\cos\theta, \tag{E.13}$$

where θ is the angle between **k** and **U**.

List of symbols/abbreviations/acronyms/initialisms

B-V	Brunt-Väisälä
DND	Department of National Defence
DRDC	Defence Research & Development Canada
DRDKIM	Director Research and Development Knowledge and Information Management
MDA	Maritime Domain Awareness
PC	Personal Computer
R&D	Research & Development
RMP	Recognized Maritime Picture
SAR	Synthetic Aperture Radar
WKB	Wentzel-Kramers-Brillouin

DOCUMENT CONTROL DATA

(Security classification of title, body of abstract and indexing annotation must be entered when the overall document is classified)

1. ORIGINATOR (The name and address of the organization preparing the document. Organizations for whom the document was prepared, e.g. Centre sponsoring a contractor's report, or tasking agency, are entered in section 8.)

London Research and Development Corporation
114 Margaret Anne Drive,
Ottawa, Ontario K0A 1L0

2. SECURITY CLASSIFICATION (Overall security classification of the document including special warning terms if applicable.)

UNCLASSIFIED
(NON-CONTROLLED GOODS)
DMC A
REVIEW: GCEC JUNE 2010

3. TITLE (The complete document title as indicated on the title page. Its classification should be indicated by the appropriate abbreviation (S, C or U) in parentheses after the title.)

The theory of internal wave wakes

4. AUTHORS (last name, followed by initials – ranks, titles, etc. not to be used)

Tunaley, J.K.E.

5. DATE OF PUBLICATION (Month and year of publication of document.)	6a. NO. OF PAGES (Total containing information, including Annexes, Appendices, etc.)	6b. NO. OF REFS (Total cited in document.)
June 2012	54	52

7. DESCRIPTIVE NOTES (The category of the document, e.g. technical report, technical note or memorandum. If appropriate, enter the type of report, e.g. interim, progress, summary, annual or final. Give the inclusive dates when a specific reporting period is covered.)

Contract Report

8. SPONSORING ACTIVITY (The name of the department project office or laboratory sponsoring the research and development – include address.)

Defence R&D Canada – Ottawa
3701 Carling Avenue
Ottawa, Ontario K1A 0Z4

9a. PROJECT OR GRANT NO. (If appropriate, the applicable research and development project or grant number under which the document was written. Please specify whether project or grant.)	9b. CONTRACT NO. (If appropriate, the applicable number under which the document was written.)
15el04	W7714-4500869967

10a. ORIGINATOR'S DOCUMENT NUMBER (The official document number by which the document is identified by the originating activity. This number must be unique to this document.)	10b. OTHER DOCUMENT NO(s). (Any other numbers which may be assigned this document either by the originator or by the sponsor.)
2012-03-001	DRDC Ottawa CR 2012-119

11. DOCUMENT AVAILABILITY (Any limitations on further dissemination of the document, other than those imposed by security classification.)

Unlimited

12. DOCUMENT ANNOUNCEMENT (Any limitation to the bibliographic announcement of this document. This will normally correspond to the Document Availability (11). However, where further distribution (beyond the audience specified in (11) is possible, a wider announcement audience may be selected.))

Unlimited

13. ABSTRACT (A brief and factual summary of the document. It may also appear elsewhere in the body of the document itself. It is highly desirable that the abstract of classified documents be unclassified. Each paragraph of the abstract shall begin with an indication of the security classification of the information in the paragraph (unless the document itself is unclassified) represented as (S), (C), (R), or (U). It is not necessary to include here abstracts in both official languages unless the text is bilingual.)

In practice, maritime surveillance includes the detection and observation of surface ships and possibly submarines, which create various types of disturbances on the sea surface. The disturbances, which form a wake, can sometimes be detected by radar, which responds to surface flows and height variations as well as slicks. The radar may be on a terrestrial platform, on an aircraft or on a spacecraft. This report focuses on the characteristics of the surface flows created by the generation of internal waves by a moving body. The treatment involves the calculation of crest patterns on the surface; it is demonstrated that these can be derived simply from the numerical solutions of a second order differential equation that describes internal waves in an internal layer with a prescribed Brunt-Väisälä profile. Though other workers have performed similar calculations, they do not describe the methodology and its details.
The numerical approach is based on a determination of eigenvectors and their eigenvalues. These represent the profiles of the waves in the layer and the horizontal wave vectors respectively. The extension to a determination of the wake wave amplitudes is outlined and the potential for the detection of submarines is discussed.
This method, which embodies simple physical models, is designed to be straightforward and expected to be a precursor to an efficient full simulation of internal wave wakes.

14. KEYWORDS, DESCRIPTORS or IDENTIFIERS (Technically meaningful terms or short phrases that characterize a document and could be helpful in cataloguing the document. They should be selected so that no security classification is required. Identifiers, such as equipment model designation, trade name, military project code name, geographic location may also be included. If possible keywords should be selected from a published thesaurus, e.g. Thesaurus of Engineering and Scientific Terms (TEST) and that thesaurus identified. If it is not possible to select indexing terms which are Unclassified, the classification of each should be indicated as with the title.)

Ship wake; internal wave

Defence R&D Canada

Canada's leader in Defence
and National Security
Science and Technology

R & D pour la défense Canada

Chef de file au Canada en matière
de science et de technologie pour
la défense et la sécurité nationale

www.drdc-rddc.gc.ca